

*Centrals*

**THE EFFECT OF STATIC MEAN STRESS  
ON THE DAMPING PROPERTIES  
OF MATERIALS**

NEAL L. PERSON  
BENJAMIN J. LAZAN

UNIVERSITY OF MINNESOTA

JULY 1956

MATERIALS LABORATORY  
CONTRACT No. AF 33(616)-2803  
PROJECT No. 7360  
TASK No. 73604

WRIGHT AIR DEVELOPMENT CENTER  
AIR RESEARCH AND DEVELOPMENT COMMAND  
UNITED STATES AIR FORCE  
WRIGHT-PATTERSON AIR FORCE BASE, OHIO

This report was prepared by the University of Minnesota under AF Contract No. AF 33(616)-2803 and covers work performed during the period of July 1954 to August 1955. The contract was initiated under Project No. 7360, "Materials Analysis and Evaluation Techniques", Task No. 73604, "Fatigue Properties of Structural Materials", and was administered under the direction of the Materials Laboratory, Directorate of Research, Wright Air Development Center, with Mr. W. J. Trapp acting as project engineer.

The authors are grateful to W. Swanson for his contribution to the work described in this report. Likewise thanks are due V. Erickson, B. Gulbrandson, D. Schultz, and H. Thomas for the drafting work and manuscript preparation.

WADC TR 55-497

Vibrational stresses resulting from near-resonant operation are often encountered in current engineering practice under conditions which superimpose static mean stresses, such as, jet engine compressor and turbine blades. One method of minimizing vibration amplitude under near-resonant operating conditions is by the use of damping. Therefore, investigation of the damping properties of materials was undertaken.

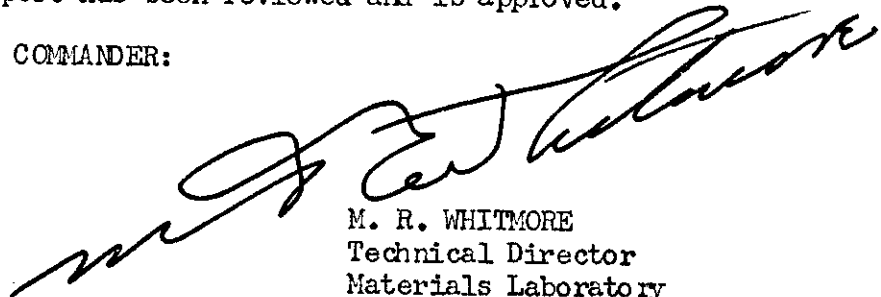
New bending vibration decay equipment was developed to determine the effect of static mean stress on the damping associated with a given alternating stress. Tests were performed on SAE 1020 steel, 2024-T aluminum, J-1 magnesium, annealed RC-55 titanium, S-816 alloy, glass laminate plastic, and 403 stainless steel. In all cases the maximum stress on the test specimens was kept below the cyclic stress sensitivity limit, below which damping is unchanged by stress history.

403 was the only material that displayed a significant change in the damping due to the superimposed static mean stress. Whereas for the other materials the change was less than 30 percent, for 403 (a magneto-mechanical alloy) the specific damping energy decreased 90 percent when the mean stress was increased from zero to 40,000 psi.

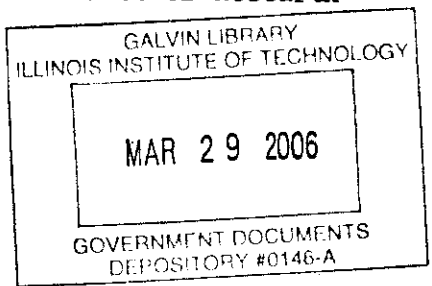
PUBLICATION REVIEW

This report has been reviewed and is approved.

FOR THE COMMANDER:



M. R. WHITMORE  
Technical Director  
Materials Laboratory  
Directorate of Research



*Centrair*  
TABLE OF CONTENTS

Section	Page
I Introduction . . . . .	1
II Test Materials and Specimens . . . . .	2
III Testing Equipment and Procedure . . . . .	2
3.1 Vibration Decay Equipment . . . . .	2
3.2 Test Procedure . . . . .	3
3.3 Reduction of Data . . . . .	4
IV Results and Discussion . . . . .	7
V Summary and Conclusions . . . . .	8
Bibliography . . . . .	9
Appendix A Sources of Energy Dissipation During the Bending Vibration Decay Test . . . . .	10
Appendix B Correlation of Bending Vibration Decay and Rotating Beam Damping Data . . . . .	12
Appendix C Definition of Symbols and Terms . . . . .	14

LIST OF TABLES

Table	Page
I Chemical Composition, Production, and Treatment . . . . .	15
II Summary of Experimental Results . . . . .	16
III Comparison of Rotating Beam and Vibration Decay Damping Data for Various Materials . . . . .	17

LIST OF ILLUSTRATIONS

Figure		Page
1	Bending Vibration Decay Damping Specimens . . . . .	18
2	Rotating Cantilever Beam Fatigue and Damping Testing Machine Adapted for Static Mean Stress Vibration Decay Tests . . . . .	19
3	Suspension System for Vibration Decay Test Equipment . . . . .	19
4	Close-Up View of Vibrating System . . . . .	20
5	Schematic Diagram of Vibration Decay Arm, Weight, and Specimen	21
6	Effect of Static Mean Stress, $S_m$ , on Specific Damping Energy for SAE 1020 Steel and RC-55 Titanium (Annealed) . . . . .	22
7	Effect of Static Mean Stress, $S_m$ , on Specific Damping Energy for 2024-T4 Aluminum and S-816 Alloy . . . . .	23
8	Effect of Static Mean Stress, $S_m$ , on Specific Damping Energy for Glass Laminate and J-1 Magnesium . . . . .	24
9	Effect of Static Mean Stress, $S_m$ , on Specific Damping Energy for Type 403 Alloy . . . . .	25
10	Comparison of Material Total Damping Energy and Air Damping Energy . . . . .	26
11	Comparison of Material Total Damping Energy and Supporting System Damping Energy . . . . .	27
12	Comparison of Material Total Damping Energy and Guide Rod Damping Energy . . . . .	28

# *Contrails*

## SECTION I. INTRODUCTION

One method of minimizing vibration amplitude under near-resonant operating conditions is by the use of damping. In some cases the only type of damping which may be effectively used is the internal damping of materials; thus, a knowledge of the damping properties of materials is required.

Vibrational stresses resulting from near-resonant operation are often encountered in current engineering practice under conditions which superimpose static mean stresses. Most of the work on damping properties of materials has been limited to the case where no static stress is present. In view of the importance of mean stress in several engineering structures (compressor and turbine blades, for example) work was undertaken on its effect on damping. Test data reported herein considers the case where the maximum stress (mean plus alternating) was kept below the cyclic stress sensitivity limit  $(1)^{1/2}$ , which is, for many materials approximately 80 percent of the fatigue limit.

Prior work on the effect of static stress on material damping has been done using the torsional vibration decay method on wire specimens with the static mean stress applied longitudinally. This method was used by Cochardt (2) (3) on several ferromagnetic materials and one nonferromagnetic material. The results of his room temperature tests showed that at lower torsional vibrational stresses the damping in ferromagnetic materials was reduced with increased tensile static stress; whereas, the damping increased with static stress for the nonferromagnetic material. It should be mentioned however that in this work the principal stress planes for the static preload (tension) were displaced  $45^\circ$  from the principal stress planes for the alternating stress (torsion). It was therefore believed desirable to procure data on the effect of mean stress under conditions in which the principal stress planes are the same for both the static prestress and the alternating stress. This is the condition present in most engineering problems, such as turbine blades for example.

The test program consisted of running bending vibration decay tests on each of the materials at various values of static mean bending stress. All tests were conducted at room temperature. The maximum total stress at the beginning of each test was kept below the cyclic stress sensitivity limit to eliminate the effect of stress history. Zero mean stress tests were run before and after the other mean stress tests to check the effect of stress history.

---

<sup>1/2</sup> Numbers in parentheses refer to references in the Bibliography.

## SECTION II. TEST MATERIALS AND SPECIMENS

The materials tested in this program were SAE 1020 steel, 2024-T4 aluminum, J-1 magnesium, annealed RC-55 titanium, S-816 alloy, glass laminate, and type 403 alloy. This particular group was selected to give a variation in material type and, therefore, in damping properties. Details on the chemical composition, processing, and heat treatment of the materials are given in Table I.

The test specimens used were designed with test sections tapered so as to produce a constant maximum stress along the outer surface under the cantilever loading (1). Specimen dimensions are given in Fig. 1.

The test sections of the specimens were prepared using the following general procedure. First the specimen stock was turned to 0.002 - 0.005 in. oversize. Next, the section was rough polished to 0.0005 in. oversize using a 240 grit belt and finally was finish polished to size using a 400 grit belt. Details of this method of polishing have been published previously (4).

## SECTION III. TESTING EQUIPMENT AND PROCEDURE

### 3.1 Vibration Decay Equipment

Since the rotating beam damping machine (1) (4) is suitable only for reversed stress work a bending vibration decay method was used for this study. A rotating cantilever machine of the type described in previous publications (1) (4) was adapted for mean stress bending vibration decay tests. A photograph of the machine is shown in Fig. 2. The general procedure was to release the specimen from a strained position and measure the rate of decay in a manner similar to that used in prior work (5) (6). As shown in prior work the rate of decay is governed by the specimen damping.

The testing machine was mounted on a 4000 pound concrete block suspended on helical springs as shown in Fig. 3. This arrangement was necessary to isolate the vibrating system from foreign vibrations. The spindle S, see Fig. 4, was clamped firmly to the table P which was clamped to the base of the machine B. The desired mean stress was produced by setting the table at a predetermined angle. When the weight arm-specimen combination was displaced



and allowed to vibrate freely it had a tendency to change its direction of motion from the displacement plane. In order to restrain the vibrations to a single plane a light rod with sharp conical ends R and a soft tension spring H were placed between the vibrating arm G and a rigid support arm C. The spring was necessary to keep the rod in contact with both arms.

The displacement of the vibrating system was recorded using a Strain Gage Amplifier-Recorder D, see Fig. 2, with a Linear Variable Differential Transformer as the transducer. The transformer core was mounted on the vibrating arm and the coil was fixed to the table. The relation between the arm displacement and the recorder displacement was found to be very nearly linear, even though the core moved through a small arc. Since the recorder used has good frequency response characteristics up to and exceeding 40 cps and none of the decay test frequencies were higher than 6 cps, the decay curves obtained were accurate recordings of the actual displacements.

The location of resultant force produced by the vibrating arm-weight system on the specimen, that is its center of percussion, was considered in the design of specimen taper. Thus the maximum stress along the test section of the specimen was essentially constant.

Air losses and the dissipation of energy in the supporting system are usually a principal cause of error in flexural vibration decay tests (7). The investigation of these and other sources of energy loss is discussed in Appendix A. As shown in this appendix the error caused by extraneous energy losses may be estimated as follows.

The air damping varies approximately from  $10^{-6}$  to  $10^{-4}$  in-lb per cycle depending on the amplitude of vibration, frequency, and size of the weight; whereas the specimen total damping energy for the various test materials range from  $5.0 \times 10^{-5}$  to  $10^{-2}$  in-lb per cycle, see Fig. 10. Therefore the maximum error in any of the tests due to air damping is about 4 percent. The supporting system energy loss, which depends on the maximum bending moment, is estimated to vary from  $10^{-6}$  to  $10^{-4}$  in-lb per cycle. From Fig. 11 it may be observed that this loss represents less than 10 percent error. Energy dissipation due to the guide rod and spring is primarily dependent on the amplitude of vibration. This loss varies approximately from  $5.0 \times 10^{-6}$  to  $3.0 \times 10^{-5}$  in-lb per cycle, which usually amounts to less than 10 percent of the total damping measurements.

As a further check on the reliability of the vibration decay method parallel tests were performed on rotating beam equipment. Those are discussed in Appendix B.

### 3.2 Test Procedure

The same general test procedure was used on all seven materials. At the beginning

of each test the maximum total stress was approximately 10 percent below the cyclic stress sensitivity limit. The tests were started by releasing the arm at the deflection corresponding to this limiting stress. A release producing a minimum of stray disturbances was obtained by fastening the deflected arm to the table with a thin wire and cutting the wire with an acetylene torch. This method of release did not excite the supporting system or produce harmonic or other stray vibration.

Tests at zero mean stress were run before and after the other mean stress tests to detect any stress history effects. Also several tests were run at each mean stress to check the reproducibility of results.

### 3.3 Reduction of Data

The conversion of experimental results to specific damping-stress data is made using the following equation<sup>1/</sup>.

$$D = \frac{\delta PX}{V_o} \frac{\sqrt{\pi} (n+2)}{2} \frac{\Gamma\left(\frac{n+2}{2}\right)}{\Gamma\left(\frac{n+1}{2}\right)} \quad \text{Eq. 1}$$

The logarithmic decrement is computed throughout the stress range tested from the equation

$$\delta = \frac{2}{N} \left( \frac{A_1 - A_N}{A_1 + A_N} \right) \quad \text{Eq. 2}$$

When  $\delta$  is less than 0.05 the error involved in this equation is less than 2 percent. If the plot of  $\log \delta$  versus  $\log$  amplitude  $A$  (or stress  $S$ ) is a straight line with a slope  $n'$ , the slope  $n$  is constant and is equal to  $n' + 2$  because both  $P$  and  $X$  vary as the first power of stress. The  $\log D$  versus  $\log S$  curve is obtained by calculating  $D$  at any given stress by use of Equation 1 and then drawing a straight line of slope  $n$  through this point. However, if the  $\log$  plot of  $\delta$  and  $A$  is not a straight line ( $n$  not constant), the specific damping energy is calculated at various stresses using Equation 1 and a smooth curve is drawn through these points. The value of  $n$  used in this case is the local value; that is,

---

<sup>1/</sup>The proof and discussion of the equations presented are given in WADC Technical Report 56-44 (not yet published) entitled "Analytical Methods for Determining Specific Damping Energy from Various Types of Tests Considering the Stress Distribution in Specimens". Refer to Appendix C for definition of symbols used.

the  $n$  used is equal to  $n'+2$ , where  $n'$  is the slope of the tangent to the  $\log \delta$  versus  $\log A$  curve at the given amplitude or stress<sup>1/</sup>.

A correction for work done by the vibrating system against gravity is required for the vibration decay equipment used in this test program. The origin of this energy loss and its determination may be determined as follows. Referring to Fig. 5, as the system vibrates, its center of gravity, point C, moves along the path BCD. The mean stress is determined by the angle  $\theta$ . Point A may be defined as the mean static position of the center of gravity during vibration between points B and D. It is observed that as the amplitude of vibration decreases, the mean position A approaches C against the force of gravity. The energy associated with this elevation of point A is subtracted from the energy in the vibrating system. Thus, the work done against gravity causes energy loss or damping in the system.

The work per cycle  $D_g$  is equal to the change in distance  $h$  per cycle, see Fig. 5, multiplied by the weight of the system  $W$ . It may be observed that

$$h = b \cos \theta \quad \text{Eq. 3}$$

but

$$b = r(1 - \cos \alpha) \quad \text{Eq. 4}$$

Therefore

$$h = r \cos \theta (1 - \cos \alpha) \quad \text{Eq. 5}$$

and the change in  $h$  per cycle

$$\Delta h = h_1 - h_2 = r \cos \theta (\cos \alpha_2 - \cos \alpha_1) \quad \text{Eq. 6}$$

Since the angle  $\alpha$  is small

$$\cos \alpha \cong 1 - \frac{\alpha^2}{2} \quad \text{Eq. 7}$$

---

<sup>1/</sup> Justification for the use of the local value of  $n$  is presented in the paper mentioned in the footnote on the previous page.

and

$$\alpha \cong \frac{a}{r} \quad \text{Eq. 8}$$

then

$$\Delta h \cong \cos \theta \left( \frac{a_1^2 - a_2^2}{2r} \right) \quad \text{Eq. 9}$$

and the work per cycle

$$D_g = \frac{W \cos \theta}{2r} (a_1^2 - a_2^2) \quad \text{Eq. 10}$$

It is observed that at  $\theta = 0$  the work is a maximum and at  $\theta = 90^\circ$  no work is done. In addition, it is seen that for  $\theta$  between  $90^\circ$  and  $180^\circ$  the correction is negative; thus, energy is added to the vibrating system.

The logarithmic decrement calculated from the decay curve must be corrected for the gravity effect before it is used in Equation 1. The observed decrement  $\delta_{og}$  is given by the equation

$$\delta_{og} = \frac{D_{og}}{2W_o} \quad \text{Eq. 11}$$

while the corrected logarithmic decrement  $\delta$ , which corresponds to the actual specimen damping, is

$$\delta = \frac{D_o}{2W_o} \quad \text{Eq. 12}$$

The material damping  $D_o$  may be expressed as

$$D_o = D_{og} - D_g \quad \text{Eq. 13}$$

Combining Equations 12 and 13

$$\delta = \frac{D_{og} - D_g}{2W_o} \quad \text{Eq. 14}$$

and referring to Equation 11, it is seen that Equation 14 becomes

$$\delta = \delta_{og} - \frac{D_g}{2W_o} \quad \text{Eq. 15}$$

## SECTION IV. RESULTS AND DISCUSSION

The effect of mean stress on damping is shown by a series of plots, Figs. 6 to 9, which show the log-log relationship between specific damping energy  $D$  and alternating stress for each of several mean stress levels. If the curves for various stress levels fall together this indicates that damping is primarily dependent on alternating stress only and is affected very little by mean stress. Separation of the lines indicates a mean stress dependence.

Figure 6 shows the results of the mean stress tests on 1020 steel. It is observed that the damping energy corresponding to any given alternating stress decreases very little with increased mean stress. At the maximum mean stress tested, 21,000 psi, a decrease of only 30 percent below the zero mean stress value is observed. This is an extremely small difference compared with the effect of alternating stress; for example, the damping at 2000 psi is only 1 percent of the value at 23,000 psi (a 21,000 psi difference).

The other test materials in which ferromagnetic damping effects are small show similar behavior, changing very little with increased prestress as shown in Table II. From this table it is seen that the maximum change in damping for all these materials is 30 percent.

RC-55 titanium was the only material which displayed a change in damping due to stress history, and this was very small. Referring to Fig. 6, the curve for zero mean stress obtained after all other tests had been completed coincided with the 9,000 psi mean stress curve. Thus, its stress history effect was less than 0.002 in-lb per cu-in per cycle at an alternating stress of 10,000 psi, which represents a decrease of less than 20 percent.

The test results for glass laminate reveal that the same damping-stress curve is obtained whether the laminations are parallel or perpendicular to the plane of vibration.

The ferromagnetic material 403 alloy shows a very significant decrease in damping with increased preload. Figure 9, which gives the test results for 403 alloy, indicates that at an alternating stress of 10,000 psi  $D$  decreased 90 percent when the mean stress was increased from zero to 40,000 psi.

The fact that type 403 alloy displayed a definite decrease in damping with increased static mean stress agrees with the results of work by Cochardt (2) (3) and may be explained by the domain theory of ferromagnetism (8). The effect of a static stress on the damping of a ferromagnetic material is similar to that of a constant magnetic field (9) (10).

The results of the tests on the five nonferromagnetic materials differ from the results obtained by Cochardt (3) who observed that significant increase in damping occurred with static stress for Refractaloy 26. This disagreement is believed to be caused by the difference

between the two testing methods. The method used by Cochardt involved a static tensile stress with superimposed alternating torsional stress, whereas, the method used in this program imposed static bending stress and alternating bending stress on the same planes. In the Cochardt tests the principal stress planes for the static stress were displaced  $45^{\circ}$  from the principal stress planes for the alternating stress, while in the case of combined static and alternating bending stresses, the principal stress planes for the two types of stress coincide.

## SECTION V. SUMMARY AND CONCLUSIONS

An adaptation of a rotating cantilever beam machine for bending vibration decay tests and the associated recording equipment are described. The use of this equipment for studying the effect of static mean stress on the damping of materials is discussed. An estimate of the error due to extraneous energy losses is given. Equation and procedure for reducing experimental results to specific damping-stress data are presented, which include the correction for energy dissipated as work against gravity.

The materials tested in this work were SAE 1020 steel, 2024-T4 aluminum, J-1 magnesium, RC-55 titanium, S-816 alloy, glass laminate, and type 403 alloy. This selection was made to provide a variety of material type and, hence, of damping properties. In all cases the tests were conducted at room temperature and below the cyclic stress sensitivity limit. The test results are presented as specific damping energy versus alternating stress curves for various mean stresses.

The following conclusions are based on the results of this investigation:

1. In the case where the maximum stress (mean plus alternating) is below the cyclic stress sensitivity limit, the effect of a static mean bending stress on the damping associated with a given alternating bending stress is small for materials with little or no magneto-mechanical effect. Materials of this type decrease in damping only 30 percent or less with increasing mean stress.
2. Increased static mean stress greatly reduces the damping of materials that have considerable magneto-mechanical damping. It is possible to decrease the specific damping energy of type 403 alloy as much as 90 percent by applying a static mean stress.

It should be emphasized that this work was conducted below the cyclic stress sensitivity limit. The magnitude of the mean stress effect was not determined at higher stress. In the region above the cyclic stress sensitivity limit however, the large effects of stress history must be carefully separated from the mean stress effects.

*Contrails*  
BIBLIOGRAPHY

1. Lazan, B. J., "A Study With New Equipment of the Effects of Fatigue Stress on the Damping Capacity and Elasticity of Mild Steel," *Trans. Am. Soc. Metals*, Vol. 42, pp. 499-558 (1950).
2. Cochardt, A. W., "Some New Magneto-Mechanical Torsion Experiments," *J. Applied Physics*, Vol. 25, No. 5, pp. 670-673 (May 1954).
3. Cochardt, A. W., "Effect of Static Stress on the Damping of Some Engineering Alloys," *Westinghouse Scientific Paper*, No. 1817, Westinghouse Research Laboratories, East Pittsburgh, Pa., March 1954.
4. Lazan, B. J. and Wu, T., "Damping Fatigue, and Dynamic Stress-Strain Properties of Mild Steel," *Proc. Am. Soc. Test. Mat.*, Vol. 51, pp. 649-681 (1951).
5. Chang, L. and Gensamer, M., "Internal Friction of Iron and Molybdenum at Low Temperatures," *ACTA Metallurgica*, Vol. 1 (1953).
6. Schabtach, C. and Fehr, R. O., "Measurement of the Damping of Engineering Materials During Flexural Vibration at Elevated Temperatures," *J. Applied Mechanics*, pp. A86-A92 (June 1944).
7. Frommer, L. and Murray, A., "Damping Capacity at Low Stresses in Light Alloys and Carbon Steel, With Some Examples of Non-Destructive Testing," *J. Inst. Metals*, Vol. 70, Part I (1944).
8. Bozorth, R. M., "Ferromagnetism," D. Van Nostrand Comp., New York, 1951.
9. Cochardt, A. W., "The Origin of Damping in High-Strength Ferromagnetic Alloys," *J. Applied Mechanics*, pp. 196-200 (June 1953).
10. Parker, E. R., "The Influence of Magnetic Fields on Damping Capacity," *Trans. Am. Soc. Metals*, Vol. 28, No. 3, pp. 661-670 (1940).
11. Kimball, A. L. and Lovell, D. E., "Internal Friction in Solids," *Physical Review*, Vol. 30, pp. 948-959 (1927).
12. Contractor, G. P. and Thompson, F. C., "Damping Capacity of Steel," *J. Iron and Steel Inst.*, Vol. 141, pp. 311-317 (1940).
13. Robertson, J. M. and Yorgiadis, A. F., "Internal Friction in Engineering Materials," *J. Applied Mechanics*, pp. A173-A182 (June 1946).
14. Demer, L. J. and Lazan, B. J., "The Effect of Stress Magnitude and Stress History on the Damping, Elasticity, and Fatigue Properties of Metallic Materials," Report on ONR Contract N8-ONR-66207, Project NR-064-361 (September 1953).

Sources of Energy Dissipation During the Bending  
Vibration Decay Test

The most serious drawback of the bending vibration decay method of determining material damping is the difficulty of eliminating extraneous energy losses. Various investigations were made to determine the approximate magnitude of the following sources of energy radiation, which are considered to be the most serious causes of error in the testing equipment developed for static mean stress work:

- (a) air
- (b) support system
- (c) guide rod and spring (see the section on test equipment)

The amount of energy dissipated due to air damping depends on the size and shape of the vibrating arm and weight, test frequency, and amplitude of vibration. Since air damping varies approximately as the square of velocity it also varies approximately as the squares of test frequency and amplitude.

The effect of air was studied in two manners. First, the damping was increased by attaching a sail-like plate of negligible weight to the arm; and secondly, the damping was decreased by running tests at reduced air pressures.

An estimate of the air damping obtained from these studies is given in Fig. 10, which also shows the total damping energy curves for each of the test materials included in the mean stress investigation. Since various types of specimens and weights were used, the total damping energy is plotted against the product of amplitude of vibration, frequency, and frontal area of the moving parts to provide a common abscissa. The air damping error at a given point on any of the material damping curves is approximately equal to the value of the air damping curve at the same value of the abscissa. It is evident from Fig. 10 that air damping contributes negligible error to tests. For example, at an abscissa value of  $10 \text{ in}^3 \text{ per sec}$ , the total damping energy for titanium, which has the lowest total damping curve of the seven materials tested, is  $1.90 \times 10^{-4} \text{ in-lb per cycle}$  while the air damping is only  $8.5 \times 10^{-6}$ . This represents an error of only about 4 percent.

The support system includes the rotating beam machine, concrete block, and suspension springs. If the block is not at resonance during the tests, no significant energy loss occurs in the supporting springs. However, if the decay test frequency is near one of the natural frequencies of the suspended block, a continuous beat transfer of motion takes



place between the vibrating arm and the block; thus the energy loss in the springs may be quite large. These critical frequencies can usually be avoided for any given material by using an appropriate combination of weight size and specimen type.

The exact location of the source of energy dissipation within the rotating beam machine is unknown. Most likely the energy loss occurs in the specimen grips and the spindle and table bearings. The grip loss is expected to depend on the tightness of the grips, but neither loosening nor tightening them causes any noticeable change in the observed damping; thus this loss is insignificant. The energy dissipation in the rotating beam machine, excluding the grips, was investigated by comparing the results of decay tests run in the rotating beam machine with the test results obtained with the same specimen fixed directly to the concrete block, as shown in Fig. 3. The approximate damping in the supporting system found by this work is shown in Fig. 11. Also shown are the total damping energy curves for the seven test materials mentioned above. In this case total damping energy is plotted against maximum bending moment since this energy loss is chiefly dependent on the moment. It may be observed from Fig. 11 that the J-1 magnesium and 2024-T4 aluminum damping curves are lowest for a given moment and therefore have the greatest error due to the support losses. At a moment of 80 lb-in, the total damping energy for magnesium and aluminum is  $8.0 \times 10^{-4}$  in-lb per cycle, whereas the supporting system damping is  $8.0 \times 10^{-5}$  in-lb per cycle.

Friction at the ends of the guide rod causes an energy loss that is dependent primarily on the amplitude of vibration and to some extent on the inertia forces in the system. Tests were run with and without the rod and spring using round specimens with flats machined on opposite sides to assure vibration in a single plane when the rod was not used. SAE 4340 steel and S-816 alloy were tested in this manner. A liberal estimate of the guide rod damping derived from this work is presented in Fig. 12 along with the total damping energy curves for the seven materials tested in the mean stress investigation. In this figure damping energy is plotted against amplitude of vibration. For the normal range of amplitude encountered, the rod damping varies from  $5.0 \times 10^{-6}$  to  $3.0 \times 10^{-5}$  in-lb per cycle; whereas for RC55 titanium, which has the lowest total damping energy associated with a given amplitude, the total damping energy varies from  $3.0 \times 10^{-5}$  to  $6.0 \times 10^{-4}$  in-lb per cycle. Thus the guide rod causes relatively small error, being less than 10 percent for the titanium tests which have the greatest error.

Correlation of Bending Vibration Decay and Rotating Beam Damping Data

As a further check on the vibration decay equipment developed for mean stress work, parallel damping tests were conducted in a rotating beam machine on a wide variety of materials. In general, the two sets of data were in close agreement as far as the damping exponent  $n$  or slope of the logarithmic damping-stress curve is concerned. However, at reversed or alternating stresses where the two damping curves overlap, the specific damping values differ considerably for some materials.

Table III lists the values of the exponent  $n$  obtained by each method for a number of materials under reversed stress. Also listed in the ratio of the specific damping from the vibration decay method to the specific damping from the rotating beam tests at a stress common to both sets of data. The comparison is made using specific damping energy and not total or average damping because only specific damping should be independent of the type of test. It is observed from Table III that for about one-half of the materials listed there was reasonably close agreement, less than 40 percent difference, between the results of the two methods. It is also seen that the vibration decay specific damping was less than the rotating beam damping for ten of the thirteen materials that display differences greater than 40 percent.

The existence of large discrepancies for certain materials and not for others suggests that one or more uncontrolled test variables are present which have a significant effect on the damping of some materials. The cyclic stress frequency is one variable that differed to a large extent between the two methods. All rotating beam damping measurements were made at 20 rpm; whereas, the vibration decay frequencies varied from 100 to 600 cpm depending on the material tested.

Several investigators have concluded from the results of their studies on a number of materials that no frequency effect exists at normal engineering stress levels (11) (12) (13). However, vibration decay tests on 2024-T4 aluminum and J-1 magnesium, both of which displayed large discrepancies between the two sets of data, showed a significant effect of frequency on the logarithmic decrement. For aluminum the decrement decreased nearly 50 percent as the frequency was increased from 450 to 1200 cpm. Likewise, the decrement for magnesium decreased approximately 50 percent as the frequency was varied from 180 to 500 cpm. A few rotating beam tests on these same two materials, mentioned in a previous publication (14), indicate that frequency may have

*Continued*

an important effect on the damping of these materials below the cyclic stress sensitivity limit. It also has been shown in an earlier publication (1) that mild steel, for which the results of the two methods were in close agreement, has no frequency effect below the cyclic stress sensitivity limit. Glass laminate, on the contrary, is one material that showed a great difference between the vibration decay and rotating beam damping data; yet, it revealed no significant variation in damping when tested over a wide range of frequencies by both the rotating beam and vibration decay methods.

Another factor which may have caused some discrepancy between the two sets of data is specimen homogeneity. Since the specimens used in the two test methods had different stress distribution, a radial variation in composition or some physical property of the test material would have a different effect on the results of the two methods. In this connection, a radial hardness gradient has been observed in some of the specimen cross sections.

The ideal procedure for comparing the two testing methods would be to run both types of tests on the same specimen at identical frequencies and under the same load conditions. However, it would be impossible to obtain satisfactory rotating beam results because the vibration decay test frequency is, of course, the lowest natural frequency of the arm and weight and if the rotating beam test speed is near or equal to this frequency, considerable flexural motion occurs. Thus, it is difficult to measure accurately the horizontal deflection of the arm caused by the presence of the hysteresis loop.

Definition of Symbols and Terms

- $A_N$  = amplitude of the  $N^{\text{th}}$  cycle of vibration, in.
- $a, b, h, r,$  = distances shown in Fig. 5, in.
- $D$  = specific damping energy of a material or that associated with a specific stress, in-lb/cu in/cycle.
- $D_g$  = energy dissipated during decay test as work against gravity, in-lb/cycle.
- $D_o$  = total damping energy absorbed by specimen per cycle, in-lb/cycle.
- $D_{og}$  =  $D_g + D_o$ , in-lb/cycle.
- $n$  = slope of log  $D$  versus log  $S$  plot =  $n' + 2$ .
- $n'$  = slope of log  $\delta$  versus log amplitude plot.
- $N$  = number of cycles of vibration.
- $P$  = normal force acting through the center of percussion necessary to produce a stress equal to the stress associated with the computed value of  $\delta$ , lb.
- $S$  = maximum stress imposed during a stress cycle, psi.
- $S_m$  = static mean stress, psi.
- $V_o$  = total effective volume of specimen contributing to dissipation of energy  $D_o$ , cu in.
- $W$  = total weight of vibration decay arm, weight and half of specimen.
- $W_o$  = total elastic energy in specimen at maximum stress, in-lb.
- $X$  = distance through which force  $P$  acts, in.
- $\delta$  = logarithmic decrement, defined as the logarithm of the ratio of successive amplitudes of decay vibrations
- $$\cong \frac{2}{N} \left( \frac{A_1 - A_N}{A_1 + A_N} \right)$$
- $\delta_{og}$  = logarithmic decrement computed from recorded decay curve.
- $\alpha$  = angle through which vibration decay arm moves from zero to maximum alternating stress.
- $\theta$  = angle between vibration decay arm at zero alternating stress and vertical direction.

# Contrails

TABLE I. CHEMICAL COMPOSITION, PRODUCTION, AND TREATMENT

Name of Material	Source	Chemical Composition, Percent	Production, Heat Treatment
SAE 1020 Steel	Crucible Steel Company Syracuse, New York	0.3 to 0.6 Mn, 0.15 to 0.25 C, 0.055 (max) S, 0.45 (max) P, (bal) Fe	Hot rolled bar stock 1-5/8 in. diameter of electric melted steel, specially controlled for uniformity and cleanliness.
2024-T4 Aluminum	Aluminum Company of America, New Ken- sington, Pennsylvania	4.30 Cu, 0.22 Fe, 0.14 Si, 0.61 Mn, 1.54 Mg, 0.01 Zn, 0.01 Cr, 0.01 Ti (bal) Al	Extruded bars 1-1/4 in. diameter, solution heat treated at 920° F, artificially aged for 24 hours at 250° F.
J-1 Magnesium	Dow Chemical Company Midland, Michigan	5.8 to 7.2 Al, 0.15 (min) Mn, 0.4 to 1.5 Zn, 0.3 (max) Si, 0.05 (max) Cu, 0.005 (max) Ni, 0.005 (max) Fe, 0.3 (max) other, (bal) Mg	Extruded bar 1-5/8 in. diameter, used in this condition
RC-55 Titanium (annealed)	Rem-Cru Titanium Inc., Midland, Pennsylvania	0.045 C, (bal) Ti	Initially forged in temperature range 1700 - 1800° F, hot rolled to 7/8 in. diameter in tempera- ture range 1450 - 1550° F and finally annealed for one hour at 1300° F.
S-816 Alloy	Allegheny Ludlum Steel Corporation, Pittsburgh, Pa.	0.397 C, 1.12 Mn, 0.50 Si, 19.62 Cr, 20.62 Ni, 4.10 Mo, 0.018 S, 0.012 P, 2.86 Cb, 4.03 W, 2.99 Fe, 42.9 Co, 1.03 Ta	3/8 in. annealed and ground, one hour at 2300° F, quenched in water, aged at 1400° F for 16 hours, furnace cooled.
Type 403 GE B50R 207 Alloy	Republic Steel <sup>1/</sup> Corporation, Cleveland, Ohio	0.12 C, 0.50 Mn, 0.12 P, 0.16 S, 0.35 Si, 12.12 Cr, 0.25 Ni, 0.04 Mo, 0.009 Al, 0.008 Sn, (bal) Fe	Electric furnace alloy hot rolled to 1 in. round. Heated to 1750° F (maintained for 15 minutes), quenched in oil. Tempered at 1050° F for 1-1/2 hours. Air cooled.
Glass Laminate Plastic	Cincinnati Testing <sup>2/</sup> and Research Labor- atory, Cincinnati, Ohio	CTL-91-LD Resin 181-114 Fiberglass	Resin impregnated into fiberglass fabric and pressed at approxi- mately 15 psi into panel 1-1/4 in. thick.

<sup>1/</sup> Procured through General Electric Company, Metallurgical Development Unit, Plant Laboratory, Building 200, Lockland 15, Ohio.

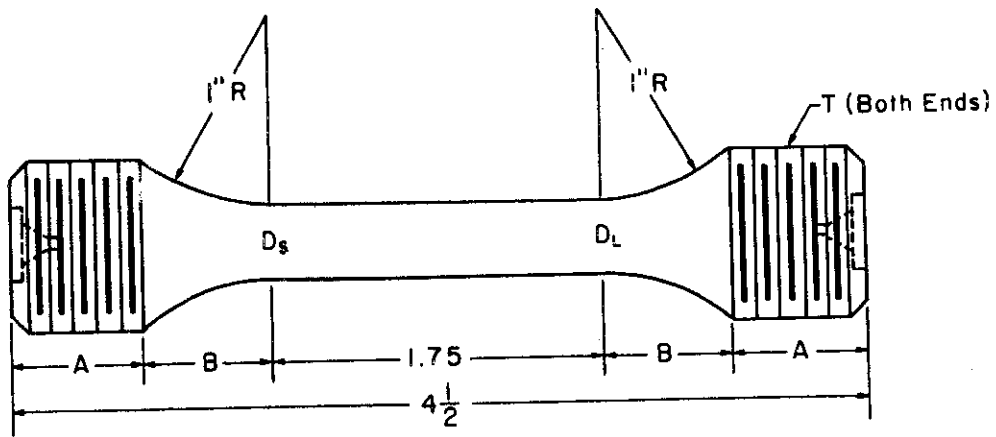
<sup>2/</sup> Procured through Wright Air Development Center, Wright-Patterson Air Force Base, Ohio, Attention: WCRTL-5, Materials Laboratory.

*Confidential*  
**TABLE II - SUMMARY OF EXPERIMENTAL RESULTS**

Material	Figure	Maximum Stress psi	Range of Mean Stress psi	Maximum Percent Decrease With Increased Mean Stress
SAE 1020 Steel	6	26,000	0-21,000	30
2024-T4 Aluminum	7	23,000	0-18,000	20
J-1 Magnesium	8	7,500	0- 6,000	10
RC-55 Titanium	6	20,000	0-15,000	30
S-816 Alloy	7	50,000	0-42,000	15
Glass Laminate	8	8,000	0- 7,000	0
Type 403 Alloy	9	50,000	0-45,000	90

TABLE III- COMPARISON OF ROTATING BEAM AND VIBRATION DECAY  
DAMPING DATA FOR VARIOUS MATERIALS

Material	Rotating Beam Slope n	Vibration Decay Slope n	Ratio of Vibration Decay Specific Damping to Rotating Beam Specific Damping
J-1 Magnesium	2.0	2.0	0.20
2024-T4 Aluminum	2.0	2.1	0.42 (at 10,000 psi)
Glass Laminate	2.4	2.1	1.80 (at 4000 psi)
RC-55 Titanium (cold-worked)	2.2	2.1	1.30 (at 10,000 psi)
RC55 Titanium (annealed)	2.0	2.0	0.31
RC130B Titanium	2.0	2.0	0.77
TP-1-2 (iron-copper alloy)	2.2	2.2	4.15
TP-1-3 (iron-copper alloy)	2.2	2.2	0.92
TP-2-B (molybdenum-tungsten)	2.0	2.0	1.20
TP-2-R (molybdenum)	2.0	2.0	2.60
Sandvik Steel (normalized)	2.6	2.5	0.42 (at 20,000 psi)
Sandvik Steel (quenched-tempered)	2.3	2.3	0.45
SAE 1020 Steel	2.2	2.1	1.00 (at 10,000 psi)
Gray Iron	2.4	2.2	1.20 (at 4,000 psi)
S-816	2.4	3.1	0.41 (at 50,000 psi)
N-155	2.5	2.2	0.57 (at 10,000 psi)
SAE 4340 Steel	2.2	2.1	0.25 (at 10,000 psi)
Type 403	2.9	2.9	0.70 (at stresses below 10,000 psi)
Gray Iron (hollow specimen)	2.2	2.0	0.89 (at 4000 psi)
SAE 1020 Steel (hollow specimen)	2.0	2.2	0.62 (at 5000 psi)
J-1 Magnesium (hollow specimen)	2.0	2.3	0.54 (at 6000 psi)
2024-T4 Aluminum (hollow specimen)	2.1	2.1	0.38
Beryllium Copper (hollow specimen)	2.3	2.3	0.76
Nodular Iron (hollow specimen)	2.2	2.1	1.25



Materials	Specimen Designation	A (in)	B (in)	D <sub>S</sub> (in)	D <sub>L</sub> (in)	T (in)
S-816, RC55 Titanium, Glass Laminate, and Type 403	AA	$\frac{11}{16}$	$\frac{11}{16}$	0.2450	0.2548	$\frac{3}{4}$ -16NF
J-1 Magnesium	AD	$\frac{9}{16}$	$\frac{13}{16}$	0.5734	0.5960	$1 \frac{3}{8}$ -12NF
2024-T4 Aluminum	D	$\frac{5}{8}$	$\frac{3}{4}$	0.5734	0.5960	$1 \frac{1}{8}$ -12NF
SAE 1020 Steel	L	$\frac{11}{16}$	$\frac{11}{16}$	0.3677	0.3820	$\frac{7}{8}$ -14NF

Fig. 1 Bending Vibration Decay Damping Specimens.



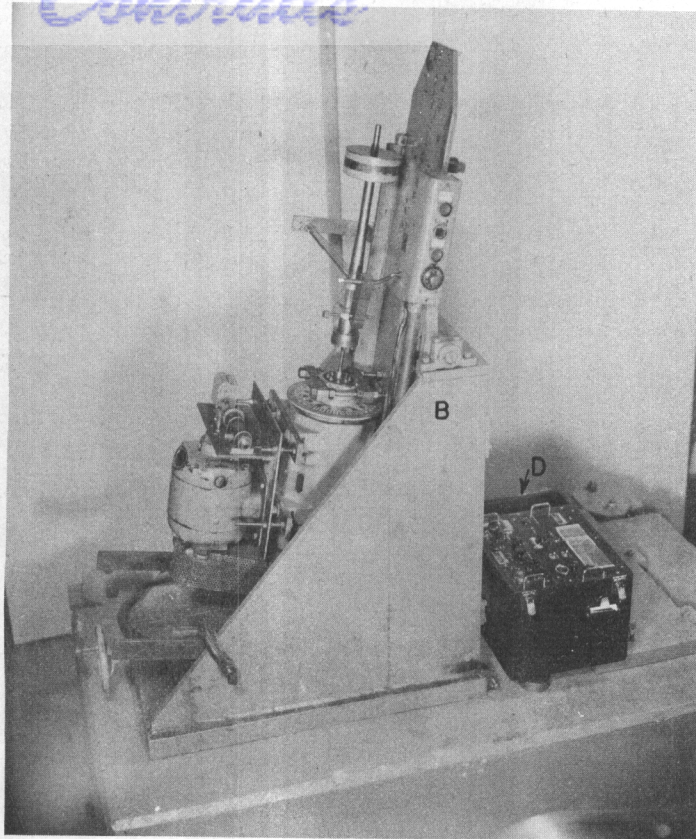


Fig. 2. Rotating Cantilever Beam Fatigue and Damping Testing Machine Adaped for Static Mean Stress Vibration Decay Tests

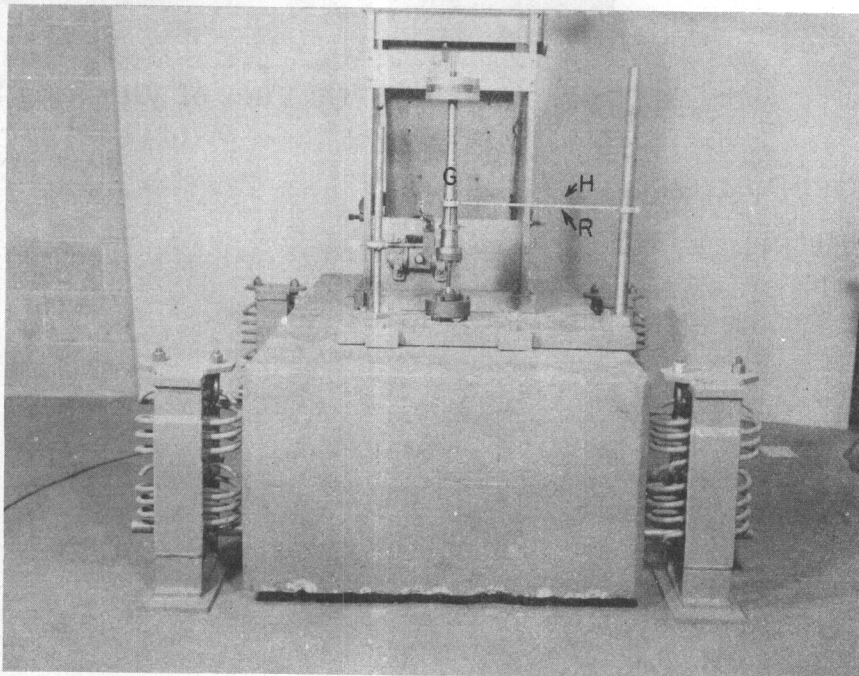


Fig. 3. Suspension System for Vibration Decay Test Equipment

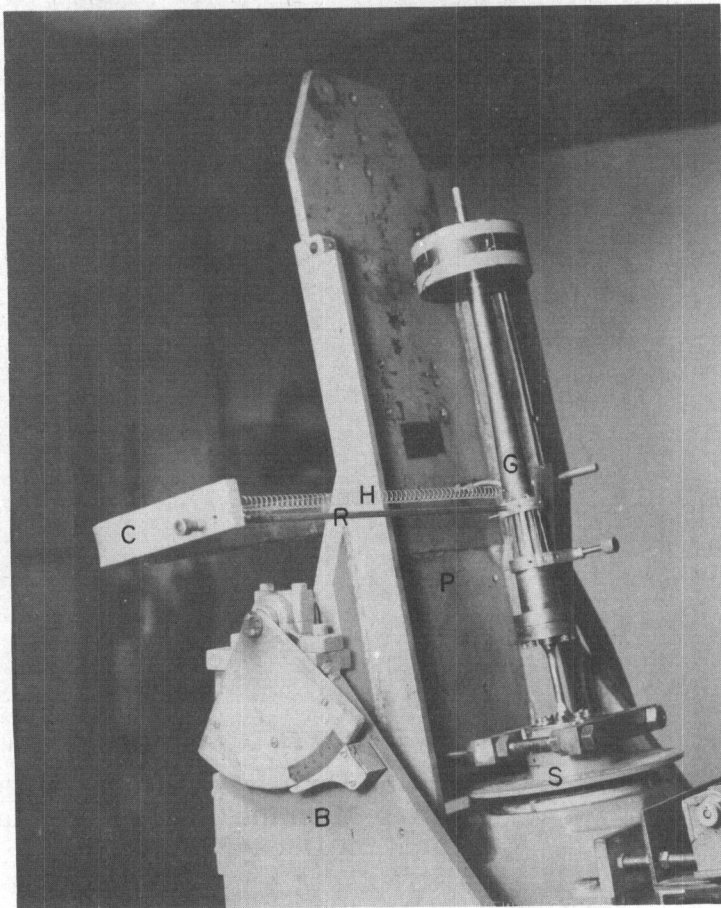


Fig. 4. Close-Up View of Vibrating System

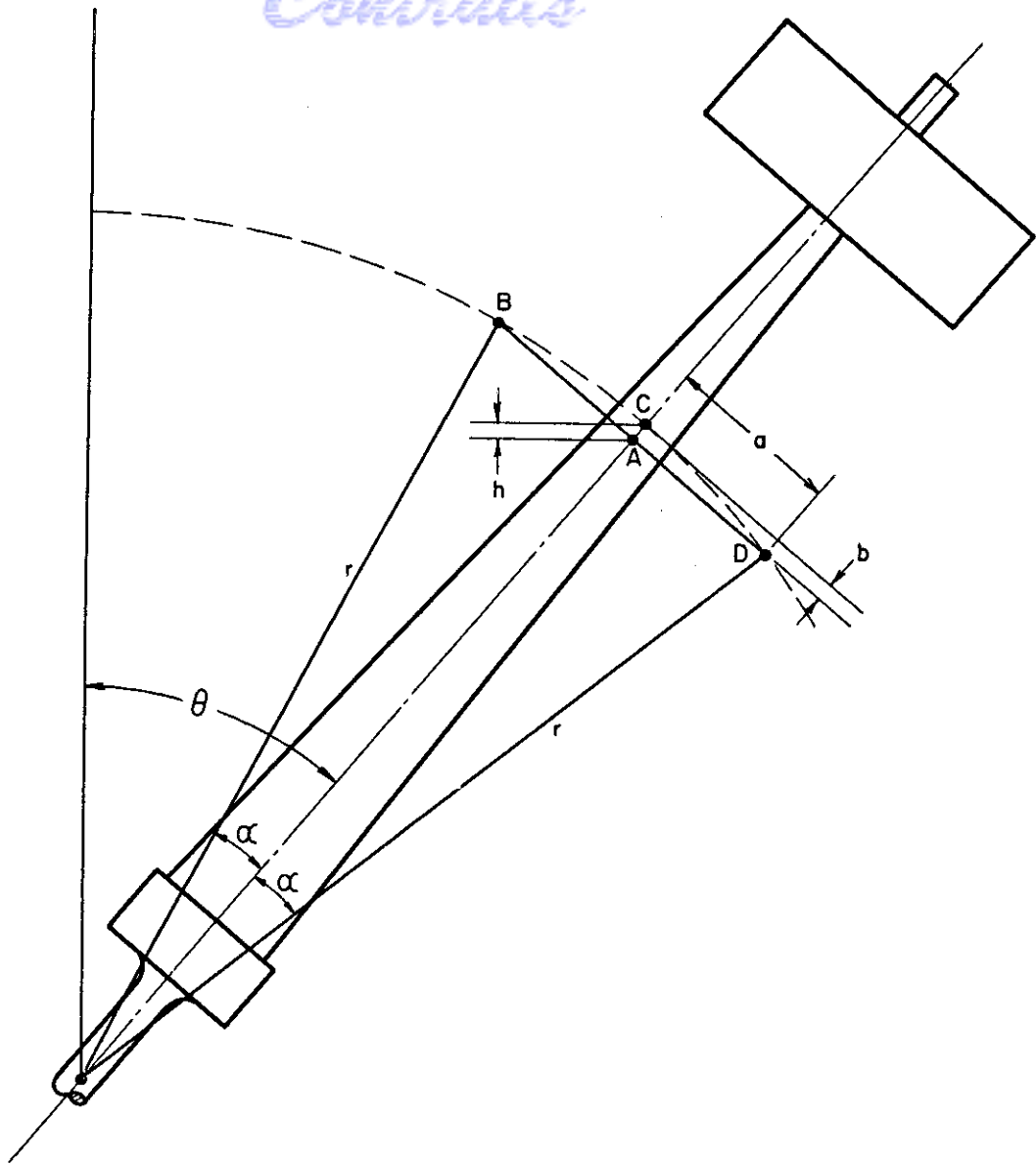


Fig. 5 Schematic Diagram of Vibration Decay Arm, Weight, and Specimen.

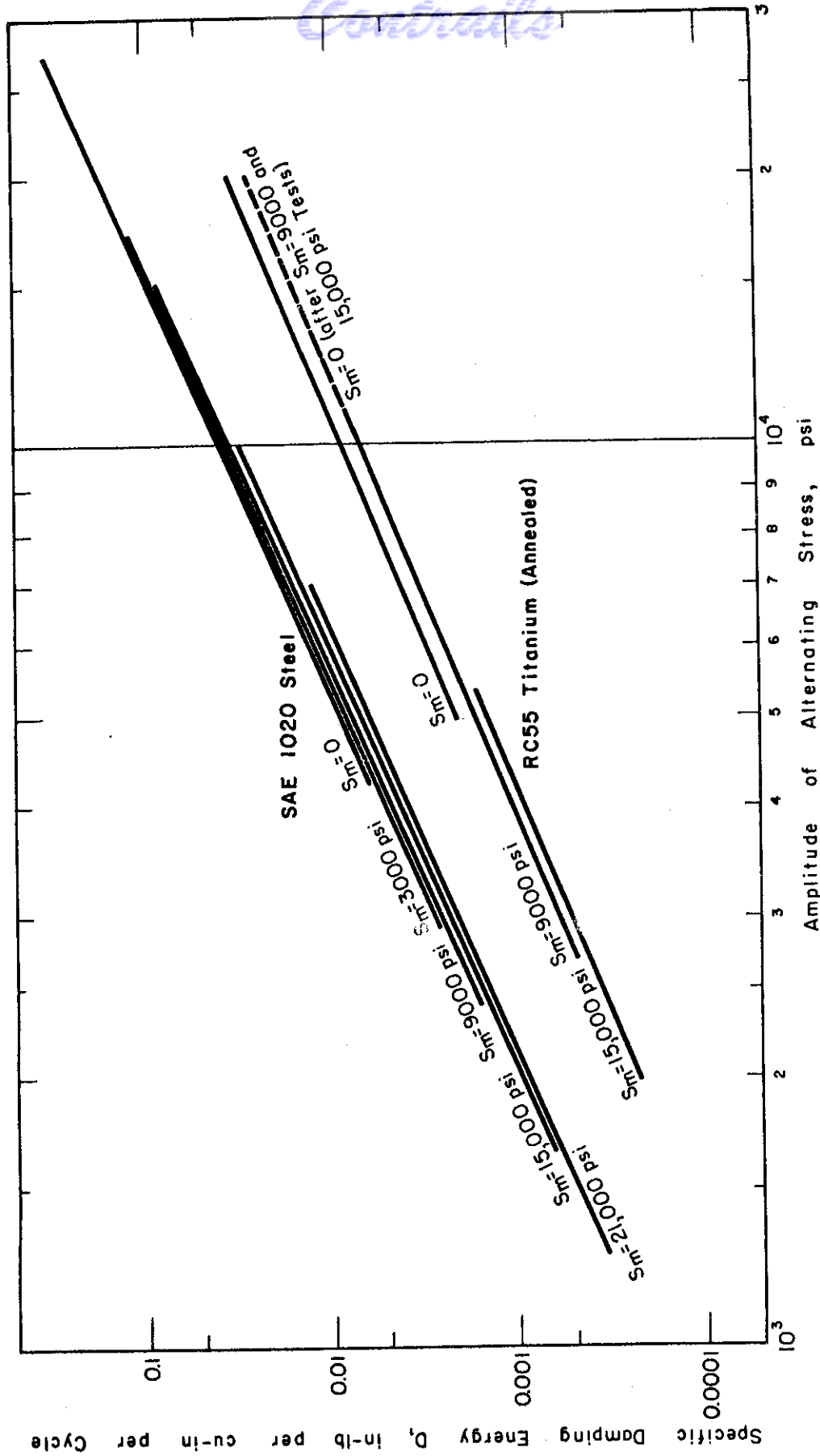


Fig. 6 Effect of Static Mean Stress,  $S_m$ , on Specific Damping Energy for SAE 1020 Steel and RC55 Titanium (Annealed).

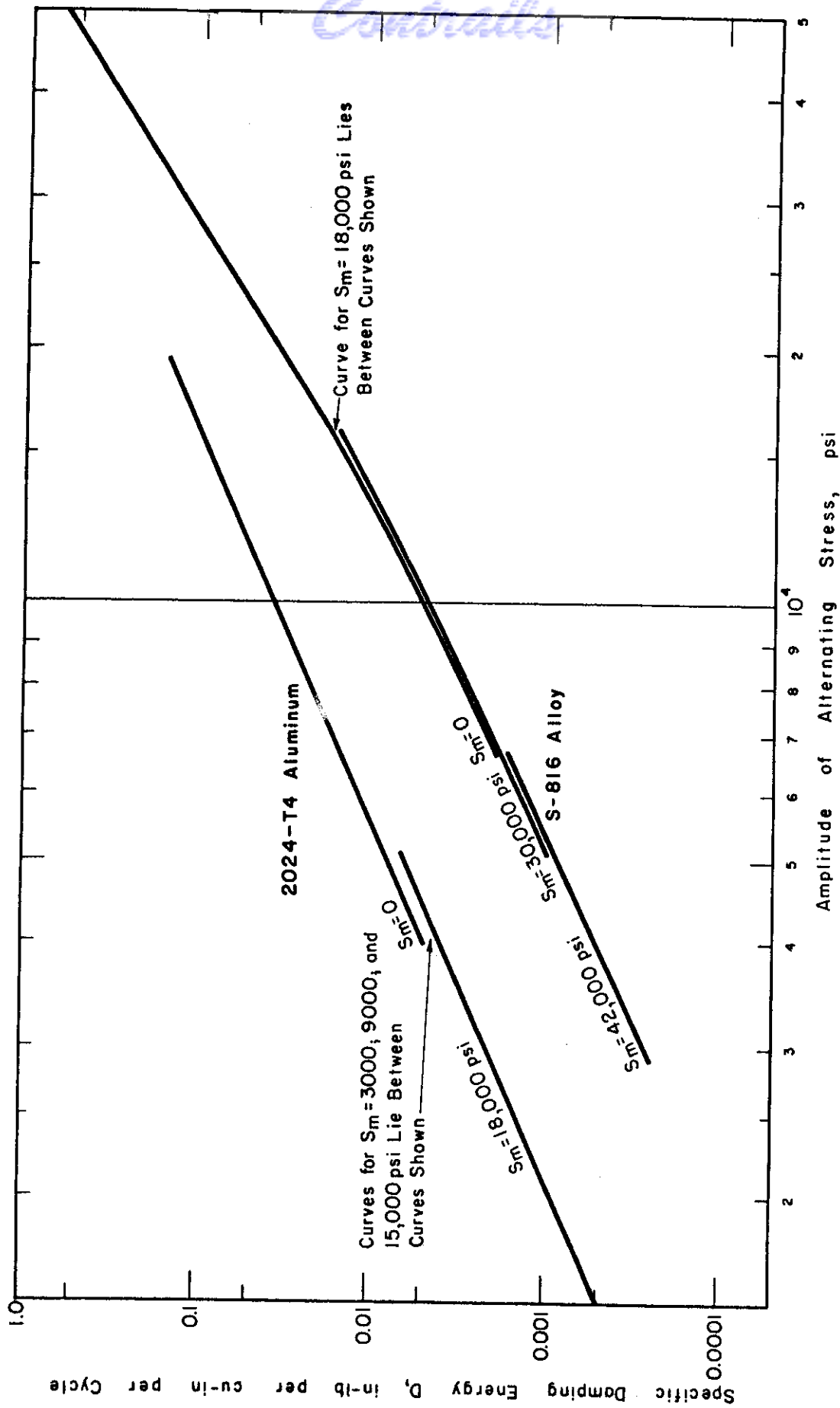


Fig. 7 Effect of Static Mean Stress,  $S_m$ , on Specific Damping Energy for 2024-T4 Aluminum and S-816 Alloy.

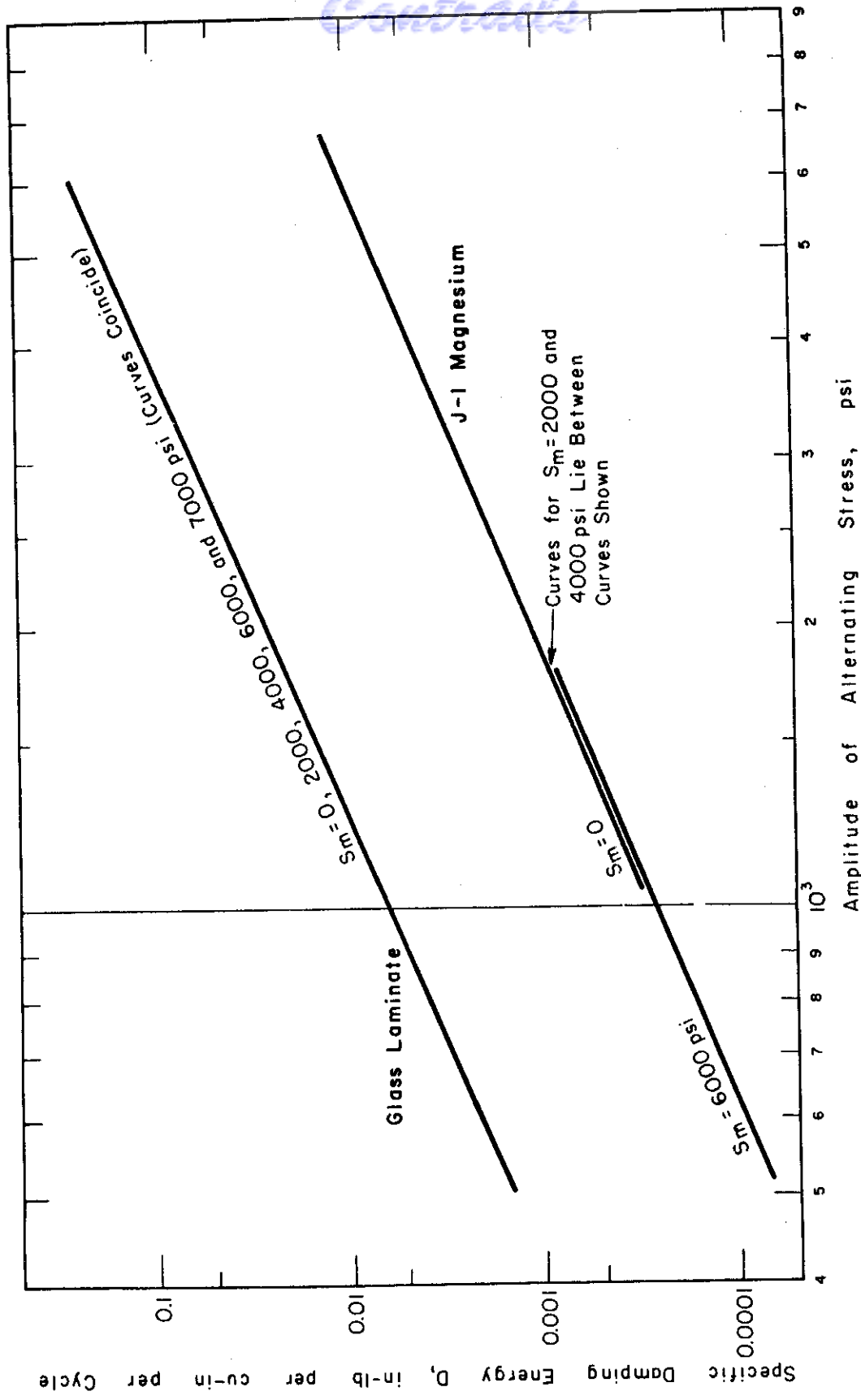


Fig. 8 Effect of Static Mean Stress,  $S_m$ , on Specific Damping Energy for Glass Laminate and J-1 Magnesium.

Contract

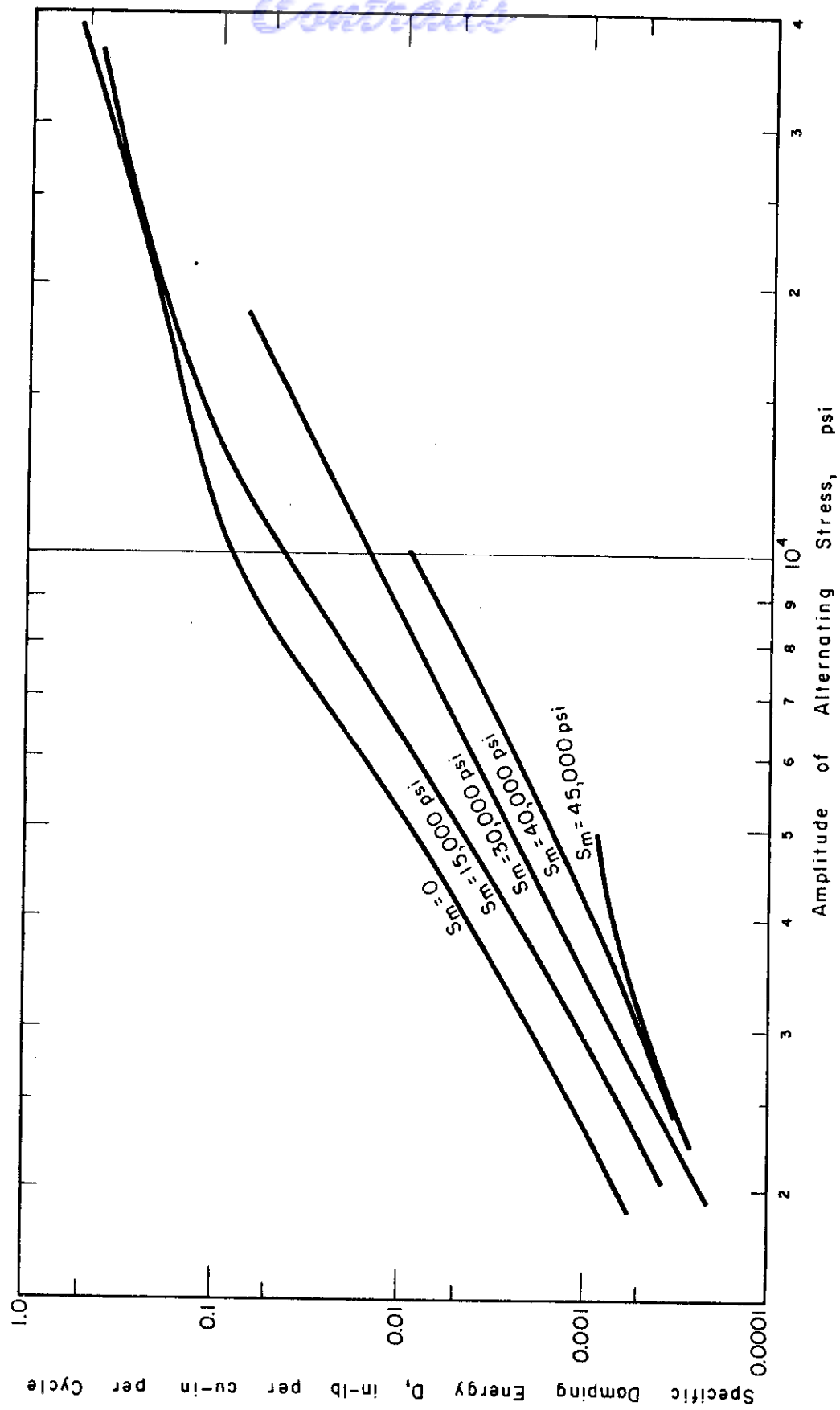


Fig. 9 Effect of Static Mean Stress,  $S_m$ , on Specific Damping Energy for Type 403 Alloy.

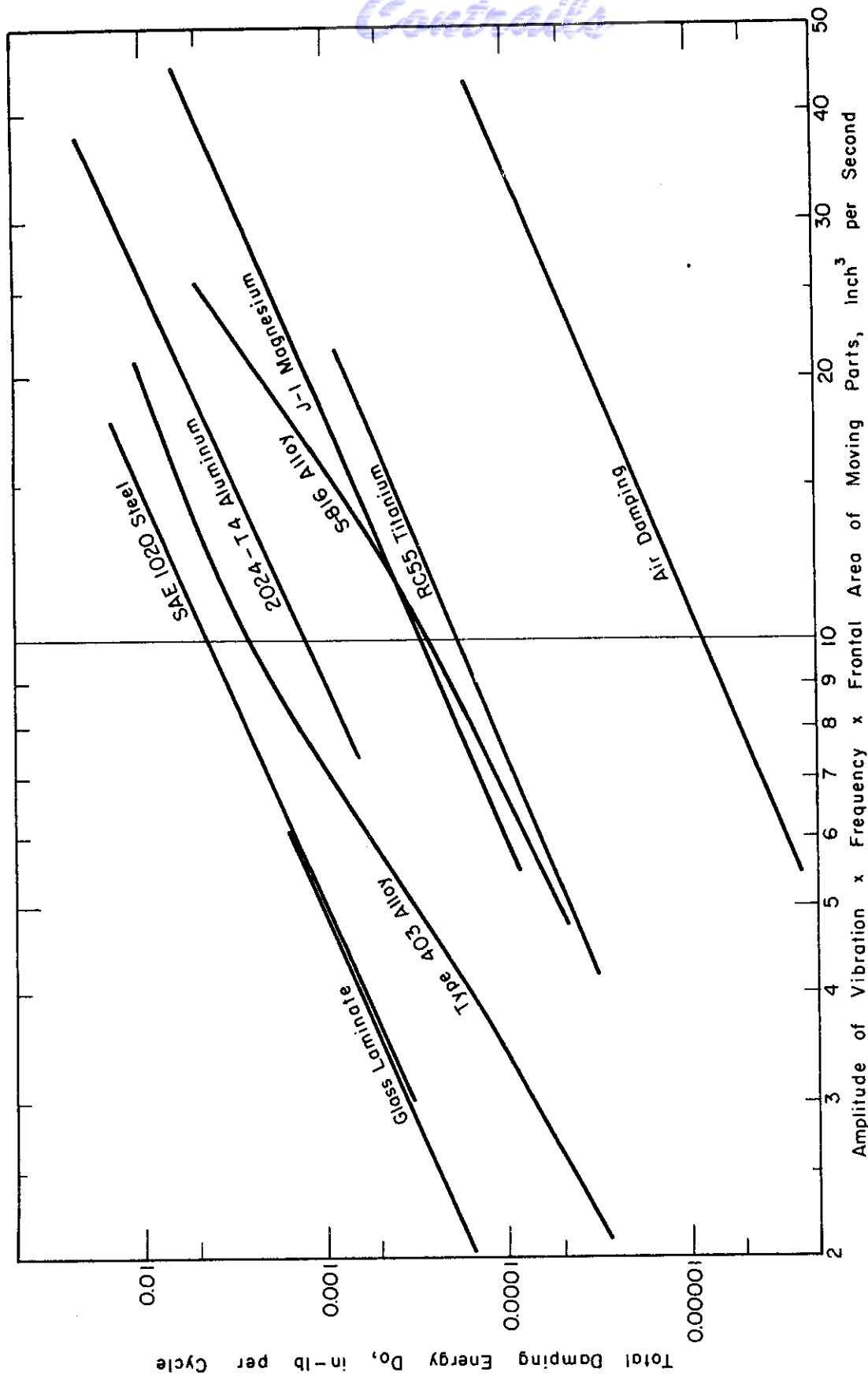


Fig. 10 Comparison of Material Total Damping Energy and Air Damping Energy.



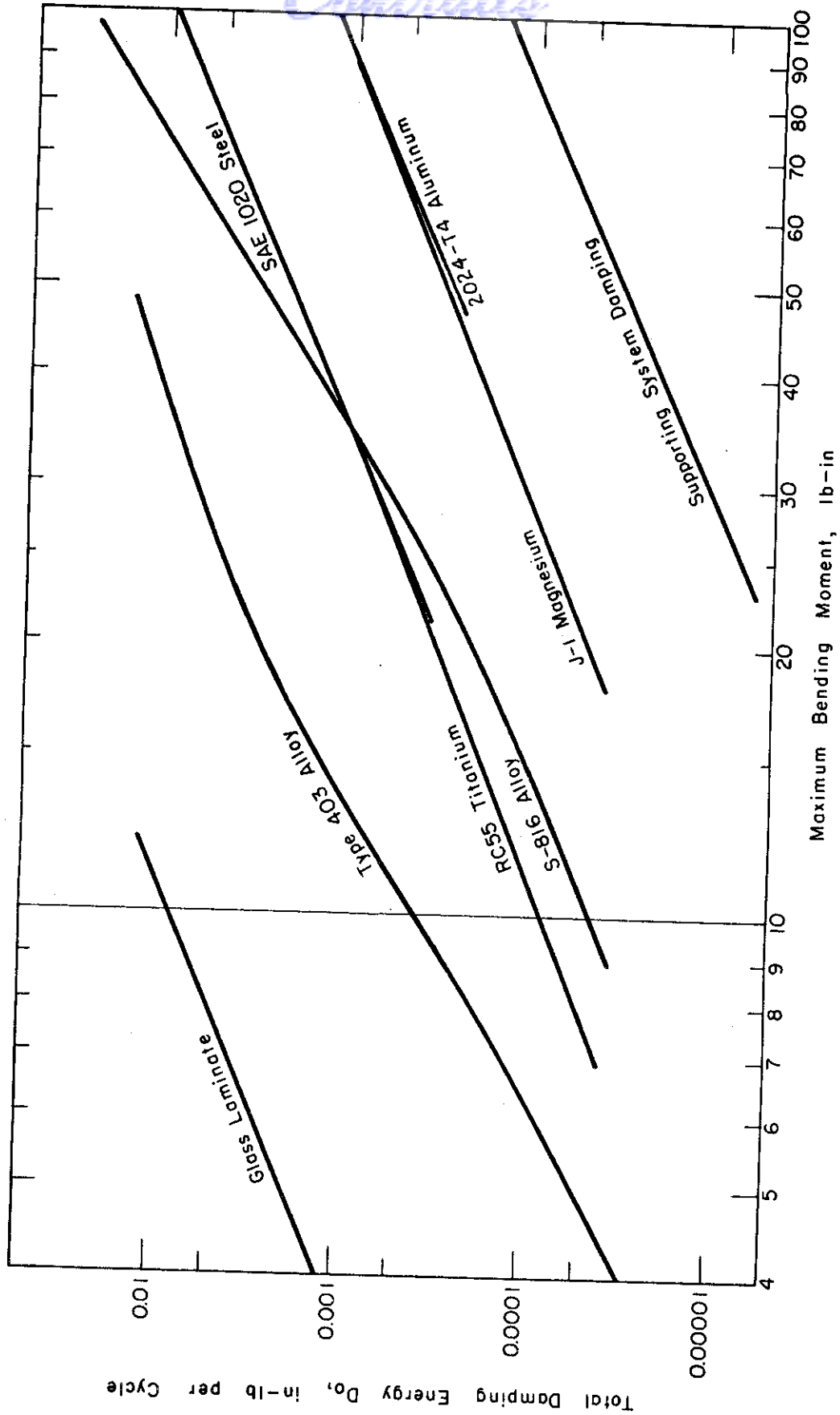


Fig. 11 Comparison of Material Total Damping Energy and Supporting System Damping Energy.

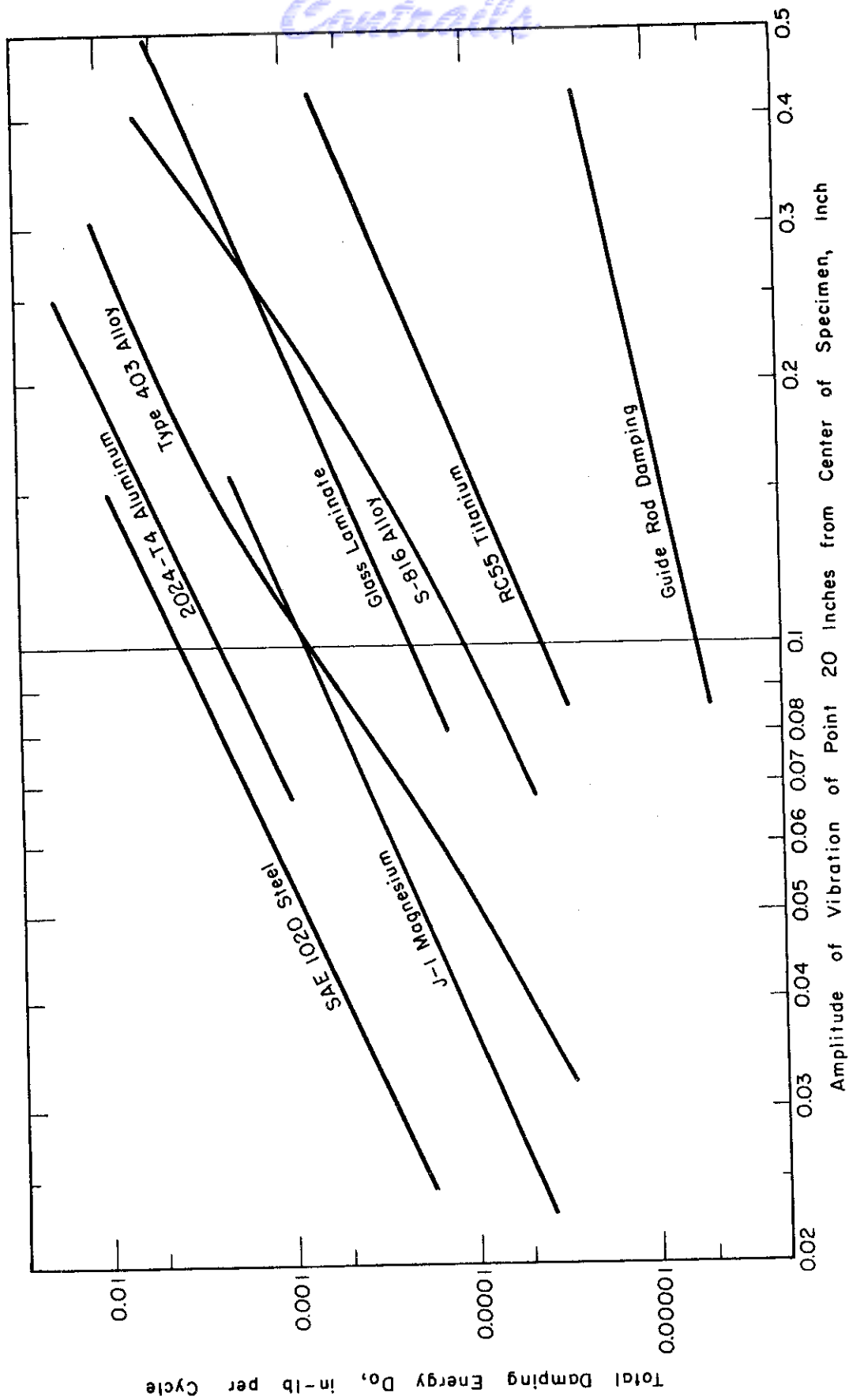


Fig. 12 Comparison of Material Total Damping Energy and Guide Rod Damping Energy.